Structural Analysis of Historical Constructions – Jerzy Jasieńko (ed)
© 2012 DWE, Wrocław, Poland, ISSN 0860-2395, ISBN 978-83-7125-216-7

DESIGN OF THE OPTIMAL FIBER REINFORCEMENT FOR MASONRY STRUCTURES VIA TOPOLOGY OPTIMIZATION

Matteo Bruggi[1], *Gabriele Milani*[2], *Alberto Taliercio*[3]

ABSTRACT

The optimal layout of the fiber reinforcement to be placed on existing masonry structures is determined using topology optimization [1]. The problem can be conveniently formulated as the minimization of the amount of reinforcement required to keep tensile stresses in any masonry element below a prescribed threshold. Strength criteria for masonry elements are provided by means of a recently presented lower bound limit analysis homogenization model [2], relying into a discretization of one-fourth of the unit cell by six CST elements. The macroscopic strength domain of masonry can be obtained in closed form, thanks to the limited number of variables involved. A multi-constrained discrete formulation that locally controls the stress field over the whole design domain [3] is adopted. The contribution presents some preliminary numerical results addressing the fiber-reinforcement of a benchmark masonry wall.

Keywords: *Masonry, Fiber-Reinforcement, Topology optimization*

1. INTRODUCTION

The use of Fiber Reinforced Polymers (FRPs) for the retrofitting of existing buildings has dramatically increased in the last decades. This technique has several advantages over standard retrofitting techniques, including flexibility, effectiveness and reversibility. Additionally, in the case of buildings in seismic regions, FRP strips do not significantly increase the structural mass and the earthquake-induced inertia forces, contrary to conventional techniques such as external reinforcements with steel plates, surface concrete coatings, and welded meshes. Laboratory tests aimed at assessing the effectiveness of FRPs in enhancing the mechanical performances of masonry structures have been recently carried out e.g. by Grande et al. [4] and Capozucca [5]. For an exhaustive and quite updated overview of the experimental researches carried out on masonry structural elements reinforced by FRPs, readers are referred to [6].

So far, the layout of the reinforcing FRP strips on laboratory samples or real structures has been basically driven by the intuition, owing to the simplicity of the loading conditions, or by the intent of healing existing cracks. A more rigorous approach relying upon structural mechanics and optimization might be necessary under complex load conditions or geometries. A preliminary attempt toward a mechanically sound design of the reinforcing path was made by Krevaikas et al. [7], who tried to identify on a rational basis the optimal layout of FRP strips on in-plane loaded masonry walls according to a strut-and-tie scheme.

In this paper, the optimal layout of reinforcing material to be placed on an existing masonry element is obtained using a rigorous approach based on topology optimization. The minimum amount (that is, the minimum cost) of reinforcement is sought, in order to keep the stress in the existing structure below a given threshold. In the optimization procedure presented hereafter, the stress over the masonry element must obey a homogenized strength criterion recently presented in [2]. Alternative choices for the objective function are possible, e.g., the highest tensile stress in the masonry element could be

[1] Assistant Professor, Politecnico di Milano, Dipartimento di Ingegneria Strutturale, bruggi@stru.polimi.it
[2] Assistant Professor, Politecnico di Milano, Dipartimento di Ingegneria Strutturale, milani@stru.polimi.it
[3] Full Professor, Politecnico di Milano, Dipartimento di Ingegneria Strutturale, talierci@stru.polimi.it

minimized, or the global stiffness (or the load bearing capacity) of the reinforced structure could be maximized.
The potentialities of the proposed approach are illustrated in Sec. 4 with reference to a technically meaningful case study.

2. HOMOGENIZED MODEL

The homogenized masonry behavior at failure is obtained by means of a simple equilibrated limit analysis model presented in [2], suitable to obtain masonry macroscopic in-plane failure surfaces at a rather limited computational effort.
The representative volume element Y (RVE, or elementary cell) depicted in Fig. 1 is considered. Y contains all the information necessary to describe the macroscopic behavior of the entire wall completely. If a running or header bond pattern is considered, as shown in Fig. 1, an elementary cell of rectangular shape can be conveniently adopted.
According to homogenization theory [8], averaged quantities representing the macroscopic stress and strain tensors ($\boldsymbol{E}$ and $\boldsymbol{\Sigma}$, respectively) are defined:

$$\boldsymbol{E} = <\boldsymbol{\varepsilon}> = \frac{1}{A}\int_Y \boldsymbol{\varepsilon}(\boldsymbol{u})dY \text{ and } \boldsymbol{\Sigma} = <\boldsymbol{\sigma}> = \frac{1}{A}\int_Y \boldsymbol{\sigma}dY \tag{1}$$

where A is the area of the 2D elementary cell, $\boldsymbol{\varepsilon}$ and $\boldsymbol{\sigma}$ stand for the local quantities (stresses and strains respectively) and <*> is the averaging operator.
The local stress ($\boldsymbol{\sigma}$) and displacement ($\boldsymbol{u}$) fields must fulfill suitable periodicity conditions that read:

$$\begin{cases} \boldsymbol{u} = \boldsymbol{E}\boldsymbol{y} + \boldsymbol{u}^{\text{per}} & \text{in} \quad Y \\ \boldsymbol{\sigma}\boldsymbol{n} & \text{anti-periodic} \quad \text{on} \quad \partial Y \end{cases} \tag{2}$$

where $\boldsymbol{u}^{\text{per}}$ is the periodic part of the displacement field, $\boldsymbol{y}$ is any point in the local reference frame (Oy_1y_2), and ∂Y is the boundary of the 2D RVE (see Fig. 1).
In this model, joints are reduced to interfaces of vanishing thickness. The units are discretized by means of a coarse mesh constituted by constant stress triangular elements (CST), as sketched in Fig. 1. In this way, and with the coarse discretization adopted, 1/4 of the RVE is meshed through 6 CST elements, indicated in Fig. 1 as 1, 2, 3, 1', 2', 3'. The generalization of the symbols to the whole cell is straightforward. In principle, block failure can occur at the brick-to-brick interfaces.
From here onwards, the superscript $^{(n)}$ will indicate any stress component belonging to the n-th element. Accordingly, assuming the wall to undergo plane-stress conditions, the Cauchy stress tensor in the n-th CST element, $\boldsymbol{\sigma}^{(n)}$, is characterized by three non-vanishing components $\sigma_{xx}^{(n)}$ (horizontal stress), $\sigma_{yy}^{(n)}$ (vertical stress) and $\sigma_{xy}^{(n)}$ (shear stress).
Referring to the static approach of limit analysis [9], equilibrium within any element is a-priori satisfied, being the stress tensor element-wise constant (div$\boldsymbol{\sigma}$ = **0**). On the contrary, two equality constraints involving stress components in adjacent triangular elements have to be prescribed at any internal interface. Consider e.g. the interface between elements1 and 2: denoting by ρ the ratio of the semi-length to the height of the brick ($\rho = b/2a$), as the stress vector must be continuous from an element to the other, the constraints $\sigma_{xx}^{(2)} = \sigma_{xx}^{(1)} + \rho\left(\sigma_{xy}^{(1)} - \sigma_{xy}^{(2)}\right)$ and $\sigma_{yy}^{(2)} = \sigma_{yy}^{(1)} + \rho^{-1}\left(\sigma_{xy}^{(1)} - \sigma_{xy}^{(2)}\right)$ hold. Similar equations must be written at the other interfaces, which are globally 28: a total of 56 equilibrium equations is obtained.
Anti-periodicity constrains for the stress vector are prescribed on the couples of triangles 1-6, 1'-6', 7-12, 7'-12', 1-7', 3-9', 4-10', 6-12', leading to additional 16 equalities. For instance, referring to couple 1-6, stress anti-periodicity amounts at setting $\sigma_{xx}^{(1)} = \sigma_{xx}^{(6)}$ and $\sigma_{xy}^{(1)} = \sigma_{xy}^{(6)}$.
Not all of the equations, however, are linearly independent. In particular, it can be shown that the corner elements 1, 6, 7 and 12 provide 4 linearly dependent equations for the shear stress.
To summarize, the optimization problem involves 73 unknowns (i.e. 72 stress components, three for each triangular element, and the load multiplier λ), 68 linearly independent equations, and a set of

inequality constraints representing the yield conditions at the interfaces and involving unknown stress components. In the framework of the lower bound theorem of limit analysis, the objective function is simply the load multiplier.

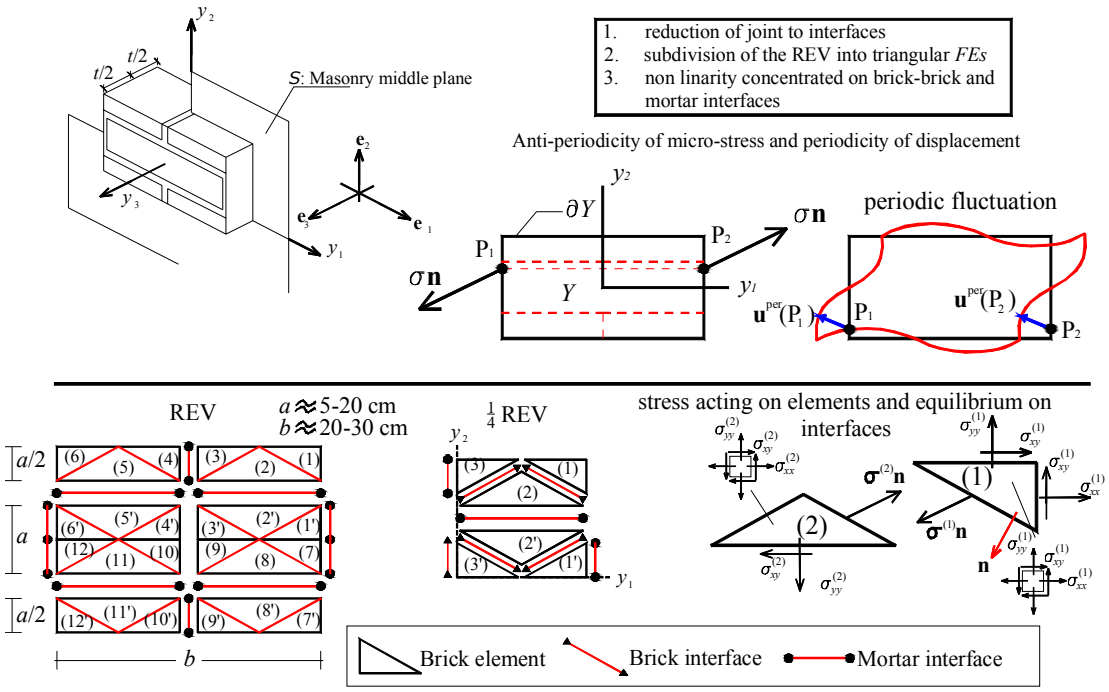

Fig. 1 The micro-mechanical model proposed. Subdivision of the REV into 24 CST triangular elements (and 1/4 into 6 elements) and anti-periodicity of the micro-stress field

To estimate a single point of the homogenized yield domain, it is thus necessary to solve the following linear programming (LP) problem:

$$\text{Find } \max \lambda \qquad \text{subject to} \begin{cases} \lambda\alpha = \dfrac{\sum_{i=1}^{24} \sigma_{xx}^{(i)} A_i}{2ab} \\ \lambda\beta = \dfrac{\sum_{i=1}^{24} \sigma_{yy}^{(i)} A_i}{2ab} \\ \lambda\gamma = \dfrac{\sum_{i=1}^{24} \sigma_{xy}^{(i)} A_i}{2ab} \\ \mathbf{A}_{eq}^{I}\mathbf{X} = \mathbf{b}_{eq}^{I} \\ \mathbf{A}_{eq}^{ap}\mathbf{X} = \mathbf{b}_{eq}^{ap} \\ f_E^i\left(\sigma_{xx}^{(i)}, \sigma_{yy}^{(i)}, \tau^{(i)}\right) \le 0, \ i = 1...24 \\ f_I^i\left(\sigma_I^{(i)}, \tau_I^{(i)}\right) \le 0, \ i = 1...32 \end{cases} \tag{3}$$

The symbols used in equation (3) have the following meaning:

- α, β and γ indicate the components of any unit vector $\boldsymbol{n}_\Sigma$, see Fig. 2, in the space of the macroscopic in-plane stresses;
- A_i is the area of the i-th element (ab/8 or ab/16);
- $\boldsymbol{X}$ is a 73×1 array, gathering all the LP problem unknowns (element stress components and load multiplier);
- $\boldsymbol{A}_{eq}^{I}\boldsymbol{X} = \boldsymbol{b}_{eq}^{I}$ is a set of linear equations collecting the equilibrium constraints at the interfaces. $\boldsymbol{A}_{eq}^{I}$ is a 56 × 73 matrix and $\boldsymbol{b}_{eq}^{I}$ is a 56 × 1 array with entries equal to zero;

- $\boldsymbol{A}_{eq}^{ap}\boldsymbol{X} = \boldsymbol{b}_{eq}^{ap}$ collects the anti-periodicity conditions and it is therefore a set of 16 equations (some of them linearly dependent). Thus $\boldsymbol{A}_{eq}^{ap}$ is a 16 × 73 matrix and $\boldsymbol{b}_{eq}^{ap}$ is a 16 × 1 array with entries equal to zero;
- $\boldsymbol{f}_E^i\left(\sigma_{xx}^{(i)},\sigma_{yy}^{(i)},\sigma_{xy}^{(i)}\right) \le \boldsymbol{0}$ is a set of possibly non-linear inequalities constraints, representing the failure surface adopted for the *i*-th element;
- $\boldsymbol{f}_I^i\left(\sigma_I^{(i)},\tau_I^{(i)}\right) \le \boldsymbol{0} \;\; \forall i = 1,...,32$ plays the role of $\boldsymbol{f}_E^i$ for the interfaces, with $\sigma_I^{(i)}$ and $\tau_I^{(i)}$ denoting the normal and shear stress acting on the *i*-th interface, respectively.

The solution of the optimization problem (3) allows a point on the homogenized failure surface to be determined, having coordinates $\Sigma_{xx} = \alpha\lambda$, $\Sigma_{yy} = \beta\lambda$ and $\Sigma_{xy} = \gamma\lambda$. Traditionally, sections of the masonry failure surface are obtained assuming a fixed angle θ of the bed joints to the macroscopic principal horizontal stress (Σ_{11}) and varying the angle $\psi = \tan^{-1}\Sigma_{22}/\Sigma_{11}$, being Σ_{22} the macroscopic vertical stress. The components of vector $\boldsymbol{n}_\Sigma$ can be expressed as:

$$\begin{cases} n_\Sigma^1 = \dfrac{1}{2}\left(\cos\psi(1+\cos(2\theta))\right) + \sin\psi(1-\cos(2\theta)) \\ n_\Sigma^2 = \dfrac{1}{2}\left(\cos\psi(1-\cos(2\theta))\right) + \sin\psi(1+\cos(2\theta)) \\ n_\Sigma^3 = \dfrac{1}{2}\left(\cos\psi - \sin\psi\right)\sin(2\theta) \end{cases} \tag{4}$$

Two typologies of interfaces are present in the model, namely brick-to-brick interfaces and mortar joints. Whereas non-linear failure surfaces may be easily dealt with within a LP scheme (abundant literature is available on this topic, see e.g. [10]), here bricks are assumed to be infinitely strong and joints are reduced to interfaces with a Mohr-Coulomb failure criterion, with tension cutoff and linear cap in compression. Hence, constituent material failure surfaces are inherently linear, and no linearization procedure is needed.

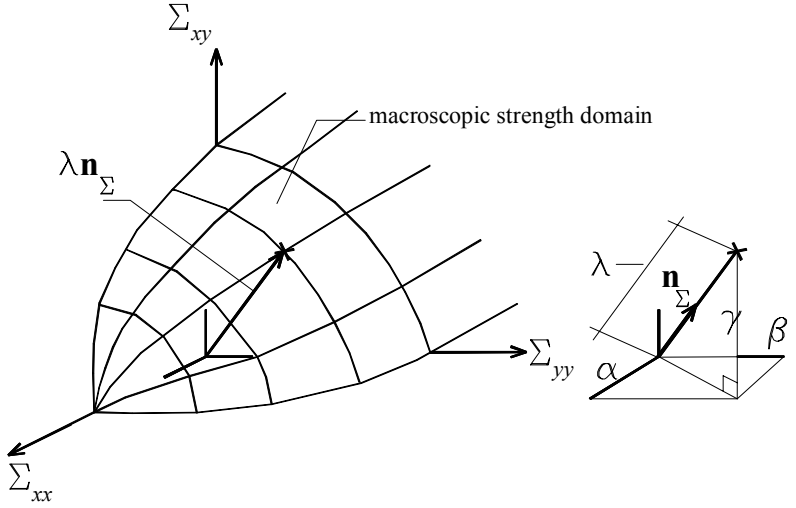

Fig. 2 General in-plane load: geometrical interpretation of the multiplier λ in the homogenized stress space ($\Sigma_{xx} = n_\Sigma^{(1)}$, $\Sigma yy = n_\Sigma^{(2)}$ and $\Sigma xy = n_\Sigma^{(3)}$)

3. TOPOLOGY OPTIMIZATION PROBLEM

Consider any masonry element subjected to prescribed loads and constraints, subjected to a plane state of stress. Assuming perfect bonding, the presence of any fiber-reinforcing layer can be taken into account adding in-plane stiffness to the underlying brickwork. A finite element discretization of the optimization problem will be derived. Extending the framework of conventional approaches for topology optimization (see e.g. [11, 12]), one may define two arrays of design variables, i.e. x_i and θ_i, representing the (normalized) density of the reinforcement and the orientation of the fibers at any element, respectively. The stiffness of the reinforced structure depends on the design variables according to the following expression:

$$\boldsymbol{K}_{Ti}(x_i, \theta_i) = \boldsymbol{K}_{Mi} + x_i^p \boldsymbol{K}_{Ri}(\theta_i), \tag{5}$$

being $\boldsymbol{K}_{Ti}$ the plane stress stiffness matrix of the i-th finite element, modeling both masonry and reinforcement. $\boldsymbol{K}_{Ti}$ includes the contribution of the underlying masonry structure, $\boldsymbol{K}_{Mi}$, along with the term accounting for the fiber-reinforcement, $\boldsymbol{K}_{Ri}$. $\boldsymbol{K}_{Ri}$ depends on θ_i, and is scaled to x_i through the so-called SIMP law that implements a penalization with exponent p, see [1]. The proposed approach allows any optimization problem to be dealt with resorting to continuous functions for the density unknowns $0 \le x_i \le 1$. The stiffness penalization at intermediate density is able to steer the solution towards the expected extreme values of the range. The terms $\boldsymbol{K}_{Mi}$ and $\boldsymbol{K}_{Ri}$ are both computed taking into account the orthotropic features of the materials. To model a fiber-reinforcement exhibiting a prevailing stiffness along a single direction, a vanishing elastic modulus is considered in the direction perpendicular to the fibers. The possible orientations of the fibers, θ_i, are unconstrained.
The optimal layout of fiber-reinforcement is defined by the distribution of reinforcing material, along with the relevant orientation of its fibers, that minimize the weight of the added phase and make the stress regime throughout the whole underlying masonry structure admissible according to the criterion defined in Sec. 2. Thus, the discrete version of the topology optimization problem can be written as: Find

$$\begin{cases} \min\limits_{\boldsymbol{x},\boldsymbol{\theta}} \sum\limits_{i=1}^{n} x_i A_i \ \text{ s.t.} \\ \left(\boldsymbol{K}_M + x^p \boldsymbol{K}_R(\boldsymbol{\theta})\right)\boldsymbol{u} = \boldsymbol{f} \\ \boldsymbol{F}_M(\boldsymbol{\sigma}_{Mj}) \le 0, \quad j = 1,...,m \\ 0 \le x_i \le 1, i = 1,...,n \\ 0 \le \theta_i \le \pi, \quad i = 1,...,n \end{cases} \tag{6}$$

The objective function in the above expression is the weight of the reinforcement, being A_i the area of the i-th finite element, x_i the corresponding density unknown, and n the number of finite elements. Recall that any element is also related to the additional optimization unknown θ_i, defining the local orientation of the fibers. Reference is also made to free material optimization for additional details on the optimal design involving anisotropic materials, see e.g. [13]. The first constraint of the optimization problem enforces the equilibrium equation for the reinforced structural element in weak form, within the framework of a classical displacement-based formulation. The global stiffness matrix may be split into two contributions related to the underlying masonry element $\boldsymbol{K}_M$ and the overlying fiber-reinforcement $\boldsymbol{K}_R$, in full agreement with the above discussion on element-wise contributions. The second requirement consists of a sets of local constraints that enforce the strength criterion presented in the Sec. 2, involving the components of the stress tensor in the masonry layer, gathered into the array $\boldsymbol{\sigma}_{Mj}$ when referring to the j-th element. This array can be computed at the centroid of each finite element, moving from the displacement and strain fields derived at equilibrium by means of a post-processing computation. All the inequalities prescribed by the adopted strength criteria are evaluated for each finite element to be constrained, whereas only a few are implemented as effective enforcements according to the selection strategy presented in [11]. This approach allows the number of active constraints to be significantly reduced, as a very limited set of local enforcements ($m << n$) may be selected and included in the optimization to provide an affordable and efficient solution of the multi-constrained minimization problem. Since stress-constraints are enforced on a fixed phase of the domain, i.e. the masonry layer, the well-known singularity problem does not affect the minimization procedure, and no relaxation is required to handle stress constraints (see e.g. [14]).
The presented optimization problem is solved by means of mathematical programming, see [15], and requires the sensitivity analysis of the objective function and the constraints on the two sets of variables, i.e. x_i and θ_i. At the beginning of the minimization process, the structural element is assumed to be evenly reinforced, which means $x_i = 1$ all over the design domain. The initial orientation of the fibers is assumed to coincide with the direction of the maximum principal stresses in the unreinforced masonry element. Indeed, the optimal fiber direction is strictly related, but not equal, to the direction of the tensile principal stresses of the underlying element. This will be further discussed in the next section.

4. NUMERICAL SIMULATIONS

A deep beam of length L = 3 m, height H = 3 m and thickness s = 250 mm, made of header bond brickwork is considered (Fig. 3a). The wall is supposed to be made of standard Italian bricks, of dimensions 250 × 120 × 55 mm^3 (length × thickness × height). The 10 mm thick joints are reduced to interfaces according to the homogenization model. The wall is fixed to the ground by means of two rigid regions at the corners of the lower side, enforcing vanishing displacements along both the horizontal and the vertical direction, and vanishing rotations. A vertical force P is distributed along the central part of the upper side of the wall. The resultant of the applied load is taken equal to 230 kN.
According to data available in the literature regarding similar panels tested up to failure [4], the Young modulus of the brickwork along the horizontal direction E_1 is taken equal to 1412 MPa, whereas the elastic modulus along the vertical direction E_2 is given a value of 1050 MPa. Additionally, the Poisson ratio is 0.1762 and the in-plane shear modulus G_{12} = 367 MPa.
The presented formulation for the topology optimization of fiber-reinforcement is implemented with the aim of distributing and orienting the minimum amount of material for an overlying layer of thickness t_F = 0.2 mm bonded to both sides of the wall, with a Young modulus E = 160 GPa along the fiber direction.
The stress state in the reinforced masonry wall must comply with the strength criterion presented in the Section 3. The mechanical properties of the constituent materials within the homogenization model are as follows: bricks are infinitely resistant; joints are reduced to interfaces obeying a Mohr-Coulomb failure criterion (cohesion = 0.1 MPa, friction angle = 30°) with tension cutoff (0.2 MPa) and a linearized compression cap (compression strength = 4 MPa, slope of the linearized cap = 60°).
Homogenized failure surface sections at different orientations of the bed joints to the principal stress Σ_{11} are depicted in Fig. 3b. Note that the behavior of the model in the tension-tension region is crucial, since optimization performed at a structural level provides reinforcement when the principal stresses in masonry exceed the tensile strength. Finally, it is worth remembering that bricks are assembled in header bond, with their maximum dimension (250 mm) disposed parallel to the side L of the wall, so that the brick length-to-height ratio is equal to 2.18. As a consequence, the orthotropy ratio, defined as the ratio of the horizontal to the vertical strength, sensibly decreases respect to a running bond pattern.

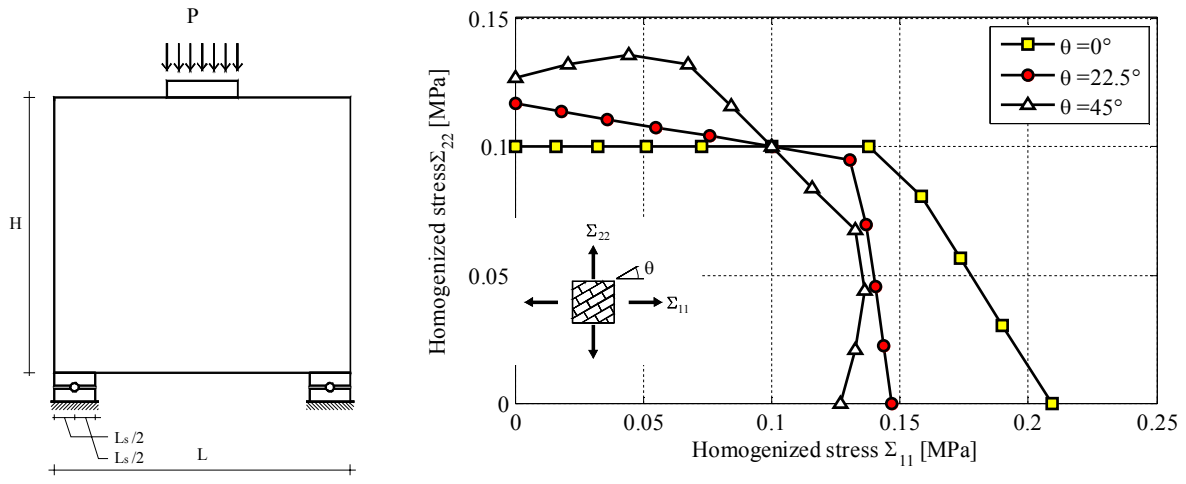

(a) (b)

Fig. 3 Geometry of the analyzed deep beam (a) and masonry homogenized failure surface sections at different orientations of the bed joints to the material axes (b)

The wall is discretized by means of about 4000 square finite elements. The minimum weight solution, admissible with respect to the selected masonry strength criterion, is summarized in Fig. 4. In particular, Fig. 4a shows the optimal distribution of fiber-reinforcing material (black regions stand for fiber-reinforced zones), whereas the optimal orientation of the fibers is depicted in Fig. 4b. Looking for regions which share a nearly homogeneous distribution in terms of fiber orientation, one may easily identify the optimal layout of FRP strips to be placed on the masonry panel. A horizontal strip should be placed at the bottom of the specimen to reduce the horizontal tensile stresses. Additionally, V-shaped stripes should be conveniently introduced to transfer a fraction of the vertical load carried by

this highly-stressed region toward the supports. Finally, in Fig. 5a contours of the difference between the optimal orientation of the reinforcing fibers and the direction of the maximum principal stress in the unreinforced element (measured in sexagesimal degrees) is plotted. Fig. 5b shows the tensile stress acting in the fiber reinforcement. As one may easily see, the optimal orientation of the fibers is related to (but not coincident with) the direction of the tensile principal stresses in the underlying panel, which may be therefore conveniently implemented to define the starting values of the entries of array θ in the optimization procedure.
The stress level in the FRP strips is compatible with the limit shear strength associated with FRP delamination, as stated by the Italian code CNR DT 200, meaning that an elastic hypothesis without limitations on the interfacial stresses between FRP and masonry material is, in this case, adequate.

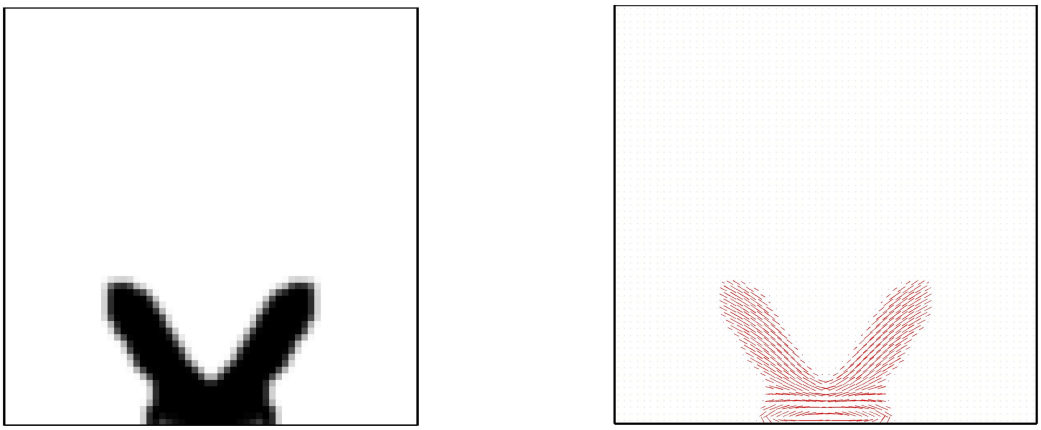

(a) (b)

Fig. 4 Optimal distribution (a) and orientation (b) of the fiber-reinforcement

5. CONCLUSIONS

An original procedure was proposed to derive the optimal layout of the fiber reinforcements to be applied to masonry structures, based on a rigorous topology optimization approach. Unlike existing procedures [7], in the proposed approach the layout of the reinforcement is completely free and no a-priori assumptions is made regarding the geometry of the reinforcing array.

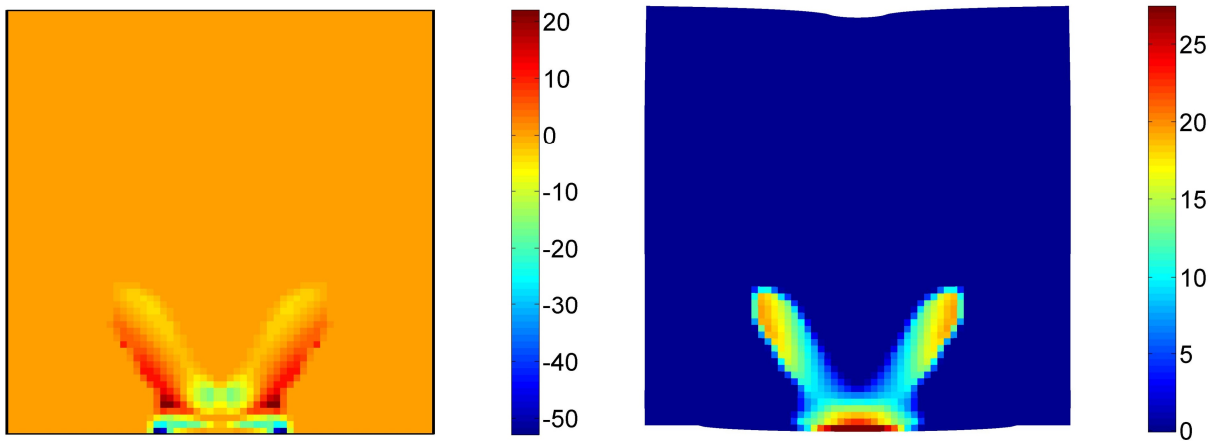

(a) (b)

Fig. 5 (a) Difference between the optimal orientation of the fibers and the direction of the maximum (tensile) principal stress in the underlying brickwork (angles measured in sexagesimal degrees), (b) Tensile stress in the FRP elements (in MPa)

The layout obtained in the example shown in Section 4 is in full agreement with the results given by energy-based optimization procedures to define equilibrated truss-like models, which can be interpreted as strut-and-tie models in concrete elements, see e.g. [15].
In many practical situations the layout of the reinforcing FRP to be placed on existing structures is basically driven by the intuition, owing to the simplicity of the loading conditions, or by the intent of

healing existing cracks. Under complex load conditions, or in presence of complex geometries, the procedure proposed in this work might turn out to be particularly appropriate for its flexibility. Existing cracks might also be taken into account in defining the geometry of the design domain. Also the choice of the objective function and the constraints can be modified, to comply with any requirements of the designer. For instance, the global structural stiffness, or its bearing capacity, could be maximized for a prescribed quantity of reinforcement, keeping the stress in the masonry element below a certain threshold.
Future perspectives of the research include the extension of the extension of the proposed procedure to multidirectional reinforcements, which are often employed in practical applications. Also, different strength criteria available in the literature for unreinforced masonry will be taken into account, and their effect on the optimal layout of the reinforcement will be assessed. Another important issue that has to be dealt with in the prosecution of the research is the control of the inter-laminar shear stresses, which are responsible for the debonding of the reinforcing layers: these stresses require structural theories more accurate than the plane stress analysis employed so far to be captured. Finally, the experimental validation of the effectiveness of the numerically obtained reinforcing layouts is envisaged.

REFERENCES

[1] Bendsøe M., Kikuchi N. (1988) Generating optimal topologies in structural design using a homogenization method. *Comp. Meth. Appl. Mech. Eng.* 71: 197-224.
[2] Milani G. (2011) Simple homogenization model for the non-linear analysis of in-plane loaded masonry walls. *Comput. Struct.* 89: 1586-1601.
[3] Duysinx P., Bendsøe M.P. (1998) Topology optimization of continuum structures with local stress constraints. *Int. J. Numer. Methods Eng.* 43: 1453-1478.
[4] Grande E., Milani G., Sacco E. (2008) Modelling and analysis of FRP-strengthened masonry panels. *Engng. Struct.* 30(7): 1842-1860.
[5] Capozucca R. (2011) Experimental analysis of historic masonry walls reinforced by CFRP under in-plane cyclic loading. *Compos. Struct.* 94: 277-289.
[6] Shrive N.G. (2006) The use of fibre reinforced polymers to improve seismic resistance of masonry. *Constr. Build. Mat.* 20(4): 269-277.
[7] Krevaikas T.D., Triantafillou T.C. (2005) Computer-aided strengthening of masonry walls using fibre-reinforced polymer strips. *Mater. Struct.* 38: 93-98.
[8] Pegon P., Anthoine A. (1997) Numerical strategies for solving continuum damage problems with softening: application to the homogenisation of masonry. *Comput. Struct.* 64(1-4): 623-642.
[9] Suquet P. (1983) Analyse limite et homogénéisation. *Comptes Rendus de l'Académie des Sciences – Série IIB – Mécanique* 296: 1355-1358.
[10] Anderheggen E., Knopfel H. (1972) Finite element limit analysis using linear programming, *Int. J. Solids Struct.* 8: 1413-1431.
[11] Bruggi M., Duysinx P. (2012) Topology optimization for minimum weight with compliance and stress constraints. *Struct. Multidiscip. Optim.*, in press.
[12] Bendsøe M.P., Sigmund O. (2003) *Topology Optimization – Theory, Methods and Applications*, Springer, Berlin.
[13] Bendsøe M.P., Guades J.M., Haber R.B., Pedersen P., Taylor J.E. (1994) An analytical model to predict optimal material properties in the context of optimal structural design. *J. Appl. Mech*. 61: 930-937.
[14] Bruggi M. (2008) On an alternative approach to stress constraints relaxation in topology optimization. *Struct. Multidiscip. Optim*. 36: 125-141.
[15] Svanberg K. (1987) Method of moving asymptotes – A new method for structural optimization. *Int. J. Numer. Methods Eng.* 24: 359-373.